Progress In Electromagnetics Research, PIER 104, 167–182, 2010

ELECTROMAGNETIC FIELD INTENSITY GENERATED BY PARTIAL DISCHARGE IN HIGH VOLTAGE INSULATING MATERIALS

A. Bojovschi, W. S. T. Rowe, and K. L. Wong

Electrical and Computer Engineering
RMIT University
Melbourne, VIC 3001, Australia

Abstract—Partial dischagre is the precursor of insulators breakdown. In this work the propagation of electromagnetic radiation emitted from partial discharge in high voltage insulating materials is investigated. Three common dielectric materials used in power industry: polymer, epoxy resin and ceramics are studied. The results obtained are envisaged to support the development of appropriate sensors for partial discharge detection. The radiation pattern is dependent on a multitude of parameters. Among these, the intensity distribution of the source as well as the dielectric material and its geometry are the main parameters. Significant differences in the radiation spectra are obtained for insulators made of ceramic material compare to non-ceramic insulators.

1. INTRODUCTION

Erosive discharges are also named Partial Discharge (PD) in high voltage (HV) technology [1, 2] and can cause failure of HV components such as capacitors, cables and inlet bushings. PD that appears inside and outside of insulating materials is a persistent problem in power industry. An internal PD is initiated in fault like cavities within insulating material while external PD occurs at the the metal-insulator interface. Both kinds of PD represent the same discharge type. This discharge is known as Townsend electron avalanches which can develop into streamers and micro-sparcs [3, 4]. Diverse electromagnetic (EM) techniques were proposed for detection and monitoring of partial discharge activity in high voltage infrastructure [5, 6]. These methods

Corresponding author: A. Bojovschi (alexe.bojovschi@rmit.edu.au).

employ EM sensors to detect the radiation emitted from PD activity and it has been shown to provide valuable information on the condition of insulators. The propagation of EM radiation in isotropic media has been well explored [7]. Furthermore the development of the Finite Difference Time Domain (FDTD) method allows an accurate investigation of EM fields in diverse dielectric media [8]. Recent works use FDTD to simulate the propagation of EM radiation emitted from PD on a distribution power line [9]. The radiation spectra along the line and in the proximity of PD source was investigated for detection purposes. Radiation spectra of PD in dielectrics showed that the EM radiation propagates in HV insulating materials as dipoles or multipoles [10]. Different radiation patterns within distinct dielectric materials correspond to a different power density. The improvement of PD detection techniques rely on an accurate interpretation of the EM spectra emitted from discharge zones. A study of coupling between the EM radiation, generated by PD, and electric or electronic systems is of real interest as novel sensing techniques use the available HV infrastructure to detect electrical faults [11]. The EM radiation emitted from PD can be characterized by its amplitude, frequency band and time of occurrence. These are determined by the rate of ionization process and the dimensions of the cavities in which a plasma discharge (also called PD) is created [12]. The repetitive break down of gas within the dielectric cavities in insulators is the main source of intense EM radiations. The PD signal is characterized by the amplitude and spectral distribution of EM signal. These characteristics together with the rate of discharge activity can assist in identifying the type of PD related fault in the HV network. PD sources are stochastic in nature. This makes difficult to obtain an exact mathematical model for the EM signal emitted by PD. Typical PD signals can be approximated numerically by a Gaussian pulse [6]. The Gaussian pulse model for PD has been used previously for simulating the EM radiation that propagates from power transformers and along HV cables [9, 10, 13, 14]. The understanding of EM radiation in power networks due to the contribution of PD activity can assist in the development of broad band fault prevention and localization systems.

In this work, FDTD is used to study the EM radiation emitted from a PD current source. The PD event was approximated by a Gaussian pulse. The radiation spectrum of the Gaussian source located within a fault cavity is investigated in three common dielectrics used in power industry: polymer, epoxy resin and ceramic. The impact of the dielectric material (HV insulator) and the cavity parameters on the radiation pattern and the power density is presented. The propagation of EM waves from cavities within different insulating

materials is assessed. The aim of this work is to improve the assessment of remaining service life of HV insulators based on their fault level reflected in the radiation pattern.

2. COMPUTATIONAL APPROACH

Defects such as cavities can be found in HV electrical insulation and dielectric materials. The gases trapped within these cavities have lower dielectric strength compare to the dielectric material. The small dielectric constant and HV in cavities facilitate the development of electron avalanches, which intensify the electric field. The ionization processes that take place in the cavity create the PD discharge. PD can last for a few nanoseconds and ultimately the breakdown of the gas in the cavity takes place. The breakdown can produce cracks in the dielectric or erosion of the cavity walls. EM radiation is also emitted. After a succession of these types of events, dielectric breakdown can occur. To be able to prevent the break down of insulators on the power network, pre-breakdown events have to be identified and investigated. This involves the analysis of the EM waves emitted due to break down of the gas within the cavities. A common way to study the propagation of EM radiation is using FDTD. This method has been used successfully to reduce the effect of EM interference and to achieve desired performance when analyzing a V transmission line line response to electromagnetic fields [15]. The FDTD method is used in this work to determine the radiation pattern emitted from PD events in HV insulating materials, originating from a fault like cavity.

2.1. Computational Method

The simulations were carried out with the FDTD method [8], using a freely available software (MEEP) package with sub-pixel smoothing for increased accuracy [16]. MEEP uses scale invariant units. The FDTD method divides space and time into a finite rectangular grids. The interaction of electric ($\mathbf{E}$) and magnetic fields ($\mathbf{H}$) with one another and with the dielectric material was modeled using Maxwells equations. The equations that were simulated to study the evolution of the fields are:

$$\frac{d\mathbf{B}}{dt} = -\nabla \times \mathbf{E} - \mathbf{J}_B - \sigma_B \mathbf{B} \tag{1}$$

$$\frac{d\mathbf{D}}{dt} = \nabla \times \mathbf{H} - \mathbf{J} - \sigma_D \mathbf{D} \tag{2}$$

$$\mathbf{B} = \mu \mathbf{H} \tag{3}$$

$$\mathbf{D} = \epsilon \mathbf{E} \tag{4}$$

where $\mathbf{D}$ is the displacement field, ε is the dielectric constant, $\mathbf{J}$ is the current density, and $\mathbf{J}_B$ is the magnetic-charge current density. $\mathbf{B}$ is the magnetic flux density, μ is the magnetic permeability, and $\mathbf{H}$ is the magnetic field. The $\mathbf{B}$ and $\mathbf{D}$ terms correspond to frequency-independent magnetic and electric conductivities, respectively. The divergence equations can be written as:

$$\nabla \cdot \mathbf{B} = -\int^t \nabla \cdot (\mathbf{J}_B(t') + \sigma_B \mathbf{B}) dt' \tag{5}$$

$$\nabla \cdot \mathbf{D} = -\int^t \nabla \cdot (\mathbf{J}(t') + \sigma_D \mathbf{D}) dt' \equiv \rho \tag{6}$$

In a more general approach ε depends not only on the position but also on the frequency and on the electric field ($\mathbf{E}$) itself. In order to discretize the the equations with second-order accuracy, FDTD technique stores different field components at different grid locations. This discretization method is known as Yee lattice [17]. The form of Yee lattice in 2D for a square cell (Δx, Δy) and a transvers electric (TE) polarization has the components of $\mathbf{E}$ stored for the edges while $\mathbf{H}$ are stored for faces. For a grid point (i, j), $x = (i\hat{e}_1 + j\hat{e}_2)\Delta x$, where $\hat{e}_k$ is the unit vector in the kth coordinate direction. The lth component of $\mathbf{E}$ is stored for the location $(i, j) + (1/2)\hat{e}_l \Delta x$. The lth component of $\mathbf{H}$ is stored at $(i + 1/2, j + 1/2) - (1/2)\hat{e}_l \Delta x$. This required the interpolation of filed components to a common point whenever the field components are combined, compared or output. Green's functions were computed to obtain the field pattern generated by PD source. The "dyadic" Green's function $G_{ij}(\omega; \mathbf{x}, \mathbf{x}')$ gives the i(th) component of $\mathbf{E}$ or $\mathbf{H}$ at $\mathbf{x}$ from a point current source $\mathbf{J}$ at $\mathbf{x}'$, such that $\mathbf{J}(x) = \hat{e}_j \cdot \exp(-i\omega t) \cdot \delta(\mathbf{x} - \mathbf{x}')$. The absorbing boundary condition used to simulate an infinite system was Perfectly Matched Layer (PML) [18]. Strictly speaking PML is not a boundary condition but rather an absorbing non-physical material that is designed to have zero reflections at its interface. When a EM wave propagates through the absorbing layer it is attenuated by absorption and it decays exponentially. In the simulations we assign to PML a finite thickness in which the absorption of EM waves gradually turns on. This is required as in actual discreet system PML has some small reflections which makes it imperfect although it is reflection-less in theoretical continuous system. For the 2D scalar wave equations the time-domain

PML equations that were solved in the x direction can be written as:

$$\frac{\partial E}{\partial t} = b\nabla \cdot H - \sigma_x E + \psi \tag{7}$$

$$\frac{\partial H_x}{\partial t} = a\frac{\partial E}{\partial x} - \sigma_x H_x \tag{8}$$

$$\frac{\partial H_y}{\partial t} = a\frac{\partial E}{\partial y} \tag{9}$$

$$\frac{\partial \psi}{\partial t} = b\sigma_x \frac{\partial H_y}{\partial y} \tag{10}$$

where E and H are the electric and magnetic fields, a and b are real and positive numbers for lossless propagating waves, σ is the conductivity and ψ is an auxiliary field variable that satisfy the equation $-i\omega\psi = b\sigma_x \frac{\partial H_y}{\partial y}$. In PML the conductivity is magnetic and electric since we have currents of electric and magnetic charges. A Gaussian impulse source with the frequency centered on 1 GHz and the width of 1 GHz was used to simulate the PD. The choice of high frequency source is based on a recent work that investigated the high frequency components in HV insulators [20]. In that work the most significant peak of the power spectrum density was observed in the frequency range from 800 MHz to 1100 MHz. The transversal electric (TE) mode is investigated in polymer, epoxy resin and ceramic materials. The amplitude and radiation spectra of EM waves that propagate from PD are studied.

2.2. Geometry of the Simulated HV Insulator Systems

The pattern of radiation depends on the structure and characteristics of the insulating material through which it propagates. The simulated system is a mathematical approximation of a insulator on a cross arm, as part of a power line system (Fig. 1). In this work only the insulators surrounded by air are presented. The simulation environment and the insulating material sample is presented in Fig. 2. The simulated dielectrics were placed in a 10 m by 10 m simulation cell. The centre of symmetry of dielectric samples corresponded with the centre of symmetry of simulation cell. The simulated geometries of insulating materials were 2D rectangular shapes with a circular cavity. The dielectric cavity where the Gaussian source is situated is located in the centre of the simulation cell. The size of the cavity is characterised by the radius r. Combinations of two different lengths (0.5 m and 1 m), three different widths (0.05 m, 0.15 m and 0.30 m) and four different radii of cavities (0.0025 m, 0.005 m, 0.0075 m and 0.01 m) are assessed. The size of the source corresponds with the diameter of the cavity. The

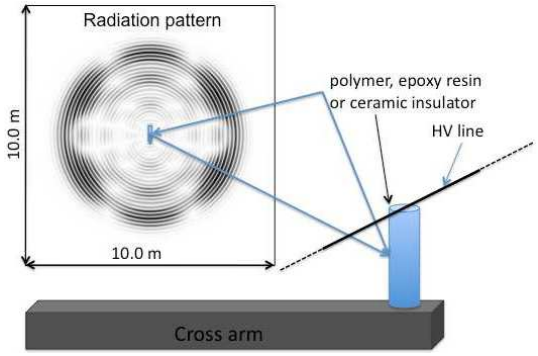

Figure 1. Schematic representation of a dielectric insulator on a cross arm and the electric field radiated by a PD in a fault like cavity situated in the centre of symmetry of the insulating material.

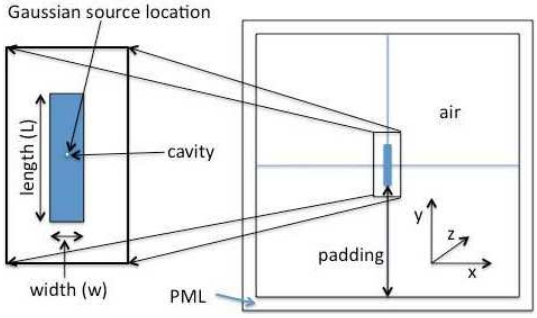

Figure 2. The simulated system is shown with the dielectric material situated in the centre. The symmetry centre of the dielectric material corresponds to the origin of the Cartesian coordinate system.

insulating material is surrounded by air. The insulating HV samples were of polymeric, epoxy resin and ceramic materials. A PML layer was used to ensure that there are no reflections of the incident radiation. In Fig. 2, the padding is considered the distance between the edge of the insulator sample and the PML in the x direction. The Gaussian current source with a width frequency of 1 GHz was placed in the centre of the simulation system which corresponds also with the centre of a cavity like fault in insulating material.

2.3. Simulation Parameters

A PD source mathematically approximated with a Gaussian source was used through out this work. The source has the centre frequency 1 GHz and a width of 1 GHz. The dielectric constant of air was $\epsilon_a = 1$. The dielectric constant of the sample insulator materials was determined experimentally previously in our laboratory using a Wayne Kerr permittivity micrometer (Type D321) [12]. Their values are $\epsilon_p = 2.984$ for polymer, $\epsilon_e = 3.772$ for epoxy resin and $\epsilon_c = 11.84$ for ceramic. The courant factor (s) was 0.5 for all the simulations. The time step (TS), defined as $\Delta t = s \cdot \Delta x$, where Δx is the spatial resolution, was 11 ps and this value was kept the same for all the simulations. The PML layer of 225 FDTD cells thick was used in all simulations. The whole simulation cell was divided in 1500 by 1500 FDTD cells. Simulations over different time scales were performed but most of the simulations presented in this work were run for 1500 time steps (TS). This was appropriate for the purpose of this work as it allows investigating the radiation spectra emitted from cavities within dielectrics. A longer time scale will be effective in studying the coupling of the EM emitted from PD with in the HV infrastructure and to study the role of possible resonances in fault like cavities within insulators. The parameters that define the geometry of system are presented in Table 1.

Table 1. The dimensions of the simulation cell and dielectric materials.

Case	x (m)	y (m)	r (m)	L (m)	w (m)
1	10	10	0.0025	0.5	0.05, 0.15, 0.30
2	10	10	0.0025	1	0.05, 0.15, 0.30
3	10	10	0.005	0.5	0.05, 0.15, 0.30
4	10	10	0.005	1	0.05, 0.15, 0.30
5	10	10	0.0075	0.5	0.05, 0.15, 0.30
6	10	10	0.0075	1	0.05, 0.15, 0.30
7	10	10	0.01	0.5	0.05, 0.15, 0.30
8	10	10	0.01	1	0.05, 0.15, 0.30

3. RESULTS

The break down events occurring in cavities within dielectrics at atmospheric pressure and temperature can happen on very different

time scales. The main parameters that affect the interval between the breakdown of gas within cavities are: the applied voltage, the size of the cavity and the dielectric strength of insulating material. These parameters are also closely related with the intensity of EM radiation emitted from insulators.

3.1. Electric Field Distribution

The results obtained in this work are used to study the EM radiation from PD activities within insulating materials. The characteristics and pattern of EM waves depend on the media through which it propagate. The simulation results of Fig. 3 for a epoxy resin and ceramic HV insulators show that the radiation propagates during the first time steps without being diffracted by the dispersive dielectric material. This regime is called a non diffractive regime and can be observed in Fig. 3 for 300th and 600th TS. This is true for short distances of propagation of a EM pulse. For longer simulation a diffractive regime takes place. This is shown in Fig. 3 for 900th, 1200th and 1500th TS. After the pulse propagates for a sufficiently long distance in the dielectric its dynamics settle into a mature dispersive regime [7, 20]. The gray scale indicates the amplitude of the displacement field which is orientated in z direction. It can be seen that in epoxy resin insulator the Gaussian source creates a field that propagates as a sequence of dipoles while in ceramic it propagates as a sequence of dipoles and quadrupoles. Detailed results on the dipole or multipole radiation which depends on the dimensions of the HV dielectrics and their dielectric constant have been presented elsewhere [10].

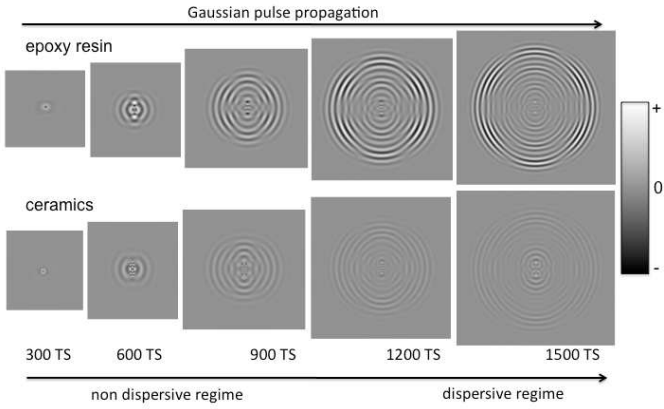

Figure 3. The distribution of E_z in and around the epoxy resin and ceramic structures at 300th, 600th, 900th, 1200th and 1500th TS.

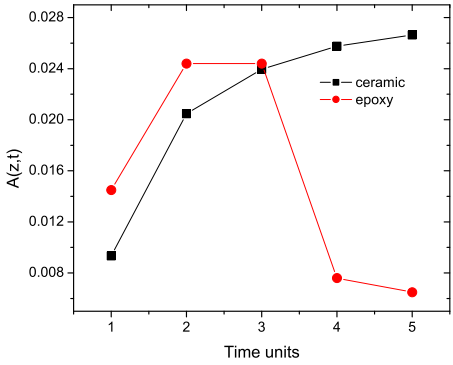

Figure 4. The intensity of E_z component of the radiation emitted from insulators as a function of time step. The dimensions of epoxy resin and ceramic samples are $L = 0.5\,\text{m}$ and $w = 0.15\,\text{m}$. The Gaussian source was situated in a cavity with radius of 0.005 m. One time unit corresponds to 300 TS.

Investigations of maximum amplitude of radiation as a function of simulation time step were performed. The maximum amplitude was determined from the entire simulation cell. As will be shown in more details in the next section the higher amplitudes for ceramics are presented within the cavity and in its proximity. For epoxy resin and polymer cases the radiation emitted by the Gaussian source exits easily the cavity and the dielectric. This is due to the dielectric constant of HV polymer and epoxy resin insulators being smaller than of ceramic materials. The results presented in Fig. 4 show that the amplitude of E_z increases during the first 900 simulation TS for both epoxy resin and ceramic. After about 900 TS the amplitude of the E_z generated by the Gaussian impulse source in the epoxy resin samples, decreases significantly as shown in Fig. 4. For the HV ceramic sample the amplitude exhibits a slight increase. This result show that for HV insulators with different dielectric constant the power density of the EM radiation is different even the characteristics of the PD fault and location are the same.

3.2. Amplitude of Electric Field in HV Insulators

The displacement field of the TE mode has higher amplitude in the cavity region that raises the mode frequency. The presence of cavities with lower dielectric strength than the surrounding dielectric material facilitates the increase of amplitudes and frequency mode. The results in Fig. 5 to Fig. 10 are presented for polymer, epoxy resin and ceramic

samples with $w = 0.15\,\text{m}$, radius of cavity $r = 0.0075\,\text{m}$ and lengths of 0.5 m and 1 m respectively. More details on the geometry were presented in Table 1. The results represent the last time step of a 1500 TS simulation. In Fig. 5 to Fig. 10 on the left is the E_z field after 150 TS and on the right and top the amplitudes of the field that corresponds to the horizontal respectively vertical lines that cross each other in the centre of the simulation cell.

In Fig. 5 from the E_z field and the amplitude evolution, it can be noted that for polymeric material the radiation propagates out from the sample easily. The amplitude of the waveform is not modified significantly by the polymeric material. As the sample increases in length Fig. 6 some radiation is trapped in the cavity although the amplitude of radiation is similar with the case when the length is $L = 0.5\,\text{m}$. The results for all the combinations presented in Table 1 show that the amplitude of radiation is similar for all the geometries. Due to space constraint and similarities in results between HV polymer insulators and epoxy resin insulators, only representative results are shown. The results for different widths of HV insulators are not presented although their influence on the radiation spectra are mentioned.

In Fig. 7 and Fig. 8, it can be seen that for epoxy resin insulator EM wave has similar magnitude to those obtained from the simulated polymeric insulator. Comparing Fig. 8 to Fig. 7 it can be noted higher amplitudes of radiation in the cavity region. They are are caused by radiation being trapped for longer time in the cavity region. In this

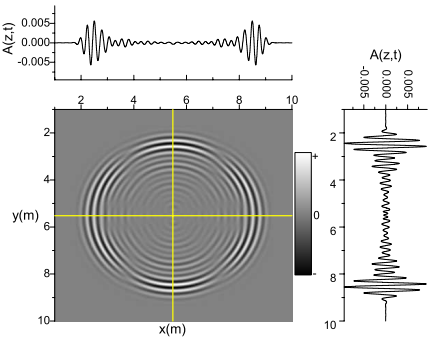

Figure 5. The E_z field evolution of a Gaussian impulse source at the 1500th TS for a polymer insulator. The length is 0.5 m, the width is 0.15 m and the cavity radius is $r = 0.0075\,\text{m}$.

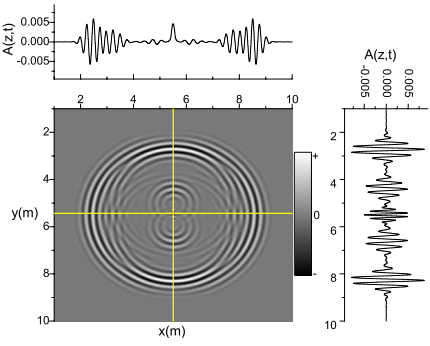

Figure 6. The E_z field evolution of a Gaussian impulse source at the 1500th TS for a polymer insulator. The length is 1 m, the width is 0.15 m and the cavity radius is $r = 0.0075\,\text{m}$.

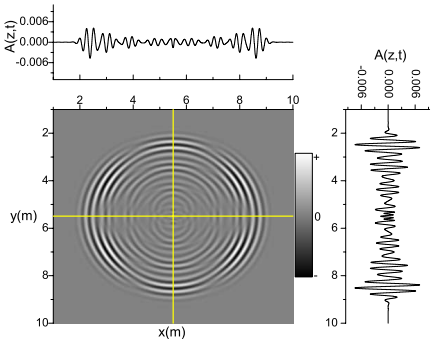

Figure 7. The E_z field evolution of a Gaussian impulse source at the 1500th TS for a epoxy resin insulator. The length is 0.5 m, the width is 0.15 m and the cavity radius is $r = 0.0075$ m.

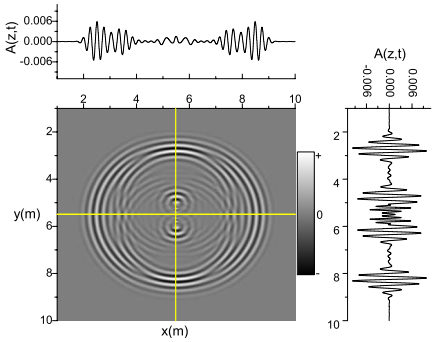

Figure 8. The E_z field evolution of a Gaussian impulse source at the 1500th TS for a epoxy resin insulator. The length is 1 m, the width is 0.15 m and the cavity radius is $r = 0.0075$ m.

case it can be observed from the E_z field that the radiation pattern depends on the size of insulating sample. Faster radiating waves can be observed from the sample with $L = 0.5$ m compare to those from a insulator of with $L = 1$ m.

The EM radiation generated by PD within cavities in ceramic dielectrics does not radiate out easily. This is due to high dielectric strength of the material. The accumulation of energy in the cavity and the small dielectric constant of air facilitate the development of waveforms with high amplitudes. It is known that the amplitude decays exponentially away from the cavity. This process can be seen in Fig. 9 and Fig. 10. For the same Gaussian source the amplitudes of EM radiation in cavities within ceramic sample are higher after 1500 TS compare to polymer or epoxy resin materials. The radiation emitted from ceramic insulators has small amplitudes compare to the amplitudes of radiation emitted from polymers and epoxy resin samples. For a sample with $w = 0.05$ m the amplitude of radiation emitted is still comparable with the amplitude in the cavity. As the dimensions of the sample increase the amplitude of radiation emitted from the cavity is significantly smaller compared with that in the cavity. These results show that the media through which it propagates influences the amplitude of the radiation emitted from a cavity. The amplitude of radiation emitted from ceramic insulators reduces significantly. The results in this work showed that less power is transmitted from a source situated in a ceramics insulator than in polymer or epoxy resin insulators.

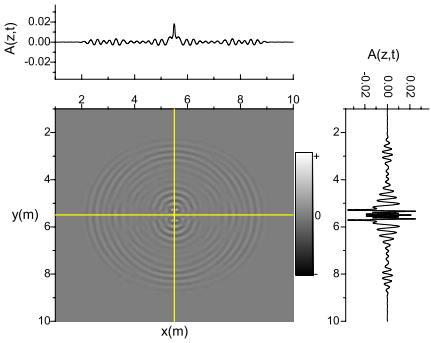

Figure 9. The E_z field evolution of a Gaussian impulse source at the 1500th TS for a ceramic insulator. The length is 0.5 m, the width is 0.15 m and the cavity radius is $r = 0.0075$ m.

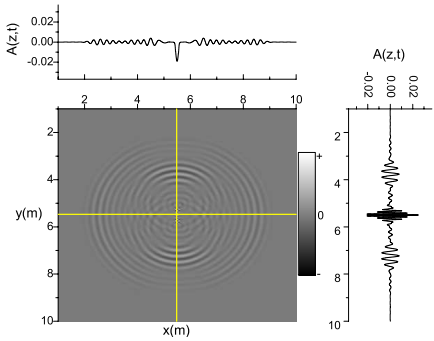

Figure 10. The E_z field evolution of a Gaussian impulse source at the 1500th TS for a ceramic insulator. The length is 1 m, the width is 0.15 m and the cavity radius is $r = 0.0075$ m.

The coupling between the EM radiation emitted from a fault, within a HV insulator or on its surface, and the HV power line has been shown to be beneficial for HV network monitoring for fault and pre-fault detection [11]. To assess the intensity of the EM radiation at the junction between the HV insulator and the power line (Fig. 1) a field monitor was placed within the simulation. The hight of the field monitor corresponds with the width of the insulator and it is placed at 0.01 m away from one end of the HV insulator. In Fig. 11 it can be seen that intensity of the EM radiation is higher for HV polymer and epoxy resin insulators than for the HV ceramic insulator. As mentioned this is a consequence of EM radiation traveling with different phase velocity in media with different dielectric constant. The results in Fig. 11 show also that the power density increases with the fault like cavity.

The dynamics of TE mode in polymer, epoxy resin and ceramic insulators shows that the parameters which determine the pattern and intensity of the radiation emitted from PD activity are: the dielectric strength of insulating material, the location of the PD source, the size of the cavity like fault situated in dielectric materials and the geometry of the insulating material. From these results it can be concluded that detecting PD on a network with mixed dielectric insulators should involve taking into account difference between the radiation emitted from different samples. This is becoming increasingly desirable as nowadays faulty ceramic insulators are replaced with polymer based insulators. Different intensity of radiation emitted from cavity like

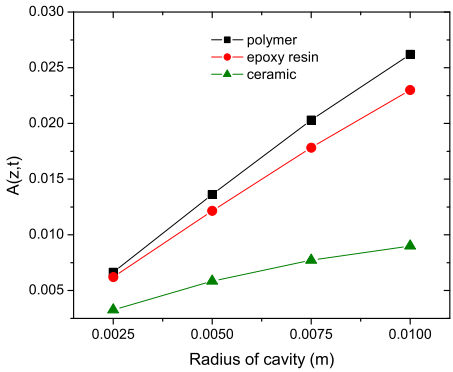

Figure 11. The amplitude of EM radiation, monitored on the extremities of HV insulators as a function of fault like cavities. The results were obtained at 1500th TS. The dimension of the samples were $L = 0.5\,\mathrm{m}$ and $w = 0.15\,\mathrm{m}$.

fault in different HV insulators can give information on their remaining life. It is of increased interest to be able to distinguish between imminent failure and acceptable discharge levels.

Experimental results that used horn antenna to determine the power spectral density of radiation emitted from PD in the three insulators mentioned above were carried out in our laboratory [20]. This work explored only the amplitude of EM radiation generated by a PD in different insulating media. The simulation systems represent a mathematical approximation of the high voltage insulators. The next step of this work incorporates the cross arm structure and the HV cable Fig. 1. From this work it can be seen that the electric field has higher amplitudes at the ends of the insulating samples. It is expected that this will result in an efficient coupling to a power line connected to the top of the insulator. The characterization of this coupling will be of benefit for developing sensing method for detecting PD in the line. This fundamental analysis is required to be undertaken for an accurate understanding of the electromagnetic flux emitted from faults in different insulating materials. The detection of PD in enclosed transformers might also be a potential extension of this study.

4. CONCLUSIONS

The radiation pattern emitted from a PD source from a fault-like cavity in a HV insulator is determined by the intensity of the source, the condition and geometry of the dielectric material. The distribution and

the amplitude of radiation were investigated. The results show that diffraction patterns are evident after more than 2000 simulation TS. The diffraction pattern depends on the geometry and characteristics of insulating materials. Representations of the E_z field allowed evaluation of the factors that contribute to different radiation patterns. The cross sectional amplitude in tandem with field investigations showed that the power generated from a PD source depends on the media in which it is located. The results show that a PD fault sensor must discriminate between EM radiation emitted from different insulators to asses their remaining service life. This is required as power densities obtained from insulating materials with different dielectric constant can indicate different levels of aging.

ACKNOWLEDGMENT

The authors would like to thank EMC Pacific Australia for providing the epoxy resin samples and acknowledges the support provided by A/Prof. Gary Bryant (RMIT University) for the dielectric constants measurements. This research was supported under Australian Research Council's Discovery Projects funding scheme (project Number DP0880770).

REFERENCES

1. Kreuger, F. H., *Partial Discharge Detection in High Voltage Equipment*, Butterworths, London, 1989.
2. Gutfleisch, F. and L. Niemeyer, "Measurement and simulation of pd in epoxy voids," *IEEE Transactions on Dielectrics and Electrical Insulation*, Vol. 2, No. 5, 729–743, 1995.
3. Ficker, T., "Electron avalanches I — Statistics of partial microdischarges in their pre-streamer stage," *IEEE Transactions on Dielectrics and Electrical Insulation*, Vol. 10, No. 4, 689–699, 2003.
4. Ficker, T., "Electron avalanches II — Fractal morphology of partial microdischarge spots on dielectric barriers," *IEEE Transactions on Dielectrics and Electrical Insulation*, Vol. 10, No. 4, 700–707, 2003.
5. Kawada, M., A. Tungkanawanich, Z. Kawasaki, and K. Matsuura, "Detection of wide-band E-M signals emitted from partial discharge occurring in GIS using wavelet transform," *IEEE Transactions on Power Delivery*, Vol. 15, No. 2, 467–471, 2000.

6. Wong, K. L., "Application of very-high-frequency (VHF) method to ceramic insulators," *IEEE Transactions on Dielectrics and Electrical Insulation*, Vol. 11, No. 6, 1057–1064, 2004.
7. Oughstun, K. E. and G. C. Sherman, *Electromagnetic Pulse Propagation in Causal Dielectrics*, Springer, Berlin, 2002.
8. Taflove, A. and S. C. Hagness, *Computational Electrodynamics: The Finite-difference Time-domain Method*, Artech House, Boston, 2000.
9. Tian, Y., M. Kawada, and K. Isaka, "Locating partial discharge source occurring on distribution line by using FDTD and TDOA methods," *IEEJ Transactions on Fundamentals and Materials*, Vol. 129, 89–96, 2009.
10. Bojovschi A., W. S. T. Rowe, and K. L. Wong, "Radiation spectra of partial discharge in dielectrics," *IEEE Proceedings of the Australian Universities Power Engineering Conference*, 1–6, Adelaide, Australia, Sep. 27–29, 2009.
11. Wong, K. L., WO 2007/070942 A1, assignee. Method and apparatus for detecting an event, International Patent patent WO 2007/070942 A1, Jun. 2007.
12. Bojovschi, A., W. S. T. Rowe, and K. L. Wong, "Dynamcis of partial discharge in dielectrics: A computational approach," *Proceedings of the 16th International Symposium on High Voltage Engineering*, 430–435, Cape Town, South Africa, Aug. 24–28, 2009.
13. Judd, M. D., L. Yang, and I. B. B. Hunter, "Partial discharge monitoring for power transformers using UHF sensors Part 1: Sensors and signal interpretation," *IEEE Electrical Insulation Magazine*, Vol. 21, No. 2, 5–14, 2005.
14. Oussalah, N., Y. Zebboudj, and S. A. Boggs, "Partial discharge pulse propagation in shielded power cable and implications for detection sensitivity," *IEEE Electrical Insulation Magazine*, Vol. 23, No. 6, 5–10, 2007.
15. Cheldavi, A. and P. Nayeri, "Analysis of V transmission lines response to external electromagnetic fields," *Progress In Electromagnetics Research*, PIER 68, 297–315, 2007.
16. Farjadpour, A., D. Roundy, A. Rodriguez, M. Ibanescu, P. Bermel, J. D. Joannopoulos, S. G. Johnson, and G. W. Burr, "Improving accuracy by subpixel smoothing in the finite-difference time domain," *Optics Letters*, Vol. 31, No. 20, 2972–2974, 2006.
17. Yee, K. E., "Numerical solution of initial boundary value problems involving Maxwell's equations in isotropic media," *IEEE*

Transactions on Antennas and Propagation, Vol. 17, 585–589, 1996.

18. Berenger, J. P., "A perfectly matched layer for the absorption of electromagnetic-waves," *Journal of Computational Physics*, Vol. 114, No. 2, 185–200, 1994.
19. Fernando, S., A. Bojovschi, W. S. T. Rowe, and K. L. Wong, "Detection of GHz frequency components of partial discharge in various media," *Proceedings of the 16th International Symposium on High Voltage Engineering*, 687–692, Cape Town, South Africa, Aug. 24–28, 2009.
20. Baldock, G. R. and T. Bridgeman, *Mathematical Theory of Wave Motion*, Halsted Press, Chichester, 1981.